

RESEARCH

Open Access



Quantitative MDCT and MRI assessment of hepatic steatosis in genotype 4 chronic hepatitis C patients with fibrosis

Gehan S. Seifeldein¹, Elham A. Hassan², Hala M. Imam³, Rania Makboul⁴, Naglaa K. Idriss⁵, Marwa A. Gaber⁵ and Reem M. Elkady^{1,6*} 

Abstract

Background: Hepatic steatosis has been shown to worsen the course of liver disease in chronic hepatitis C (CHC) patients, and it may reduce the efficacy of antiviral therapy and accelerate disease progression. In this cross-sectional study, we aimed to evaluate the role of multidetector computed tomography and magnetic resonance imaging (MRI) in the quantitative assessment and grading of hepatic steatosis to evaluate the association between hepatic steatosis and fibrosis in Egyptian genotype 4-CHC (G4-CHC) patients.

Results: Histopathological hepatic steatosis was found in 70.3% of 155 patients. No correlation was found between the CT ratio and pathological hepatic steatosis. Proton density fat fraction, T1-fat fraction, and fat percentage correlated with histological steatosis grading ($r=0.953, p<0.001$; $r=0.380, p=0.027$ and $r=0.384, p=0.025$, respectively). An agreement between steatosis grading by histology and 1H-MRS was found in 74.2% of patients. Compared to other MRI modalities, proton density fat fraction had the highest area under the receiver operating characteristic curve (AUC), with 0.910, 0.931, and 0.975 for mild, moderate, and severe steatosis, respectively. The cutoff with the best ability to predict steatosis was >4.95 for a proton density fat fraction (AUC = 0.958) with 95.8% sensitivity, 90% specificity, 78.5% positive predictive value, and 96.1% negative predictive value.

Conclusion: 1H-MRS had good diagnostic performance in predicting hepatic steatosis in G4-CHC patients, and hence, it may offer a useful noninvasive quantitative modality for grading steatosis with clinical applicability, especially in those where a liver biopsy cannot be done.

Keywords: Liver, Steatosis, MDCT, 1H-MRS, Fibrosis, Biopsy

Background

Intracellular fat accumulation (steatosis) is a common feature in different liver diseases [1]. Steatosis is the histological hallmark of non-alcoholic fatty liver disease (NAFLD) but also may occur with alcohol abuse, viral hepatitis, HIV and genetic lipodystrophies, and chemotherapy [2]. Studies have shown that 5–15% of patients with NAFLD present with established cirrhosis on liver

biopsy [3, 4] and about 5% of individuals with isolated steatosis eventually developed cirrhosis [5].

Hepatic steatosis is so frequent histological feature (30–70%) among chronic hepatitis C (CHC) patients compared with patients with other chronic hepatitis that it is considered of diagnostic significance [6, 7]. Hepatic steatosis has been shown to worsen the course of liver disease in CHC patients, and it may reduce the efficacy of antiviral therapy and accelerate disease progression [8, 9]. Furthermore, steatosis reduces hepatocellular functional reserve and contributes to postoperative hepatic failure after liver transplantation or resection [8]. Previous

*Correspondence: reem.elkady@aun.edu.eg

¹ Present Address: Department of Radiology, Faculty of Medicine, Assiut University, Assiut, Egypt

Full list of author information is available at the end of the article

reports suggest that HCV infection changes the expression profile of lipid metabolism-associated factors in the liver and lipid accumulation in hepatocytes may be due to a direct effect of HCV, especially genotype 3 (G3) [10, 11]. Insulin resistance and steatosis are independent predictors of impaired response to antiviral treatment in chronic hepatitis C [10]. Thus, assessment of hepatic steatosis in CHC patients for clinical care requires not only diagnosis but also grading of its severity.

Non-targeted percutaneous liver biopsy with direct histological visualization is the current gold standard to diagnose hepatic steatosis. However, liver biopsy is an invasive maneuver with a lack of representation of the whole liver in a few samples. Moreover, most of the diffuse liver diseases are inherently heterogeneous renders biopsy suffering from sampling variability [12]. For measuring hepatic steatosis and reducing unneeded liver biopsy, multidetector computed tomography (MDCT) and magnetic resonance imaging (MRI) are noninvasive tools that allow both qualitative and quantitative assessment of fat content [13]. Previous studies investigated the quantification of hepatocellular lipid content (HCL) using MRI and MDCT in G3-CHC patients [14, 15]. The highest prevalence of HCV infection is present in Egypt, with the majority of patients (92.5%) infected with genotype 4 (G4) [16]; therefore, in this study, we aimed to evaluate the role of MDCT and MRI in the quantitative assessment and grading of hepatic steatosis in Egyptian G4-CHC patients also to evaluate the association between hepatic steatosis and fibrosis.

Methods

Patients

Between February 2015 and June 2018, a single-center cross-sectional study included 200 treatment-naive G4-CHC patients, who were candidates to receive antiviral therapy, recruited from Internal Medicine and Tropical Medicine clinics in our institution. They had to be between 18 and 70 years old and scheduled for liver biopsy. CHC was identified as persistent or intermittent elevation in alanine transaminase (ALT) or aspartate transaminase (AST) levels for more than 6 months with the presence of anti-HCV antibodies and positive serum HCV RNA [17].

Patients with evidence of alcohol abuse, diabetes mellitus, HBV co-infection, HIV co-infection, liver cell failure, hepatic focal lesions, splenectomy, any contraindication for MRI, e.g., the presence of a cardiac pacemaker, any contraindication for CT such as pregnancy or any contraindication of the liver biopsy were excluded from the study.

A total of 200 G4-CHC patients were consecutively recruited to this study. Forty-five patients were excluded

as follows: eight patients had claustrophobia for MRI examination, 17 patients had newly discovered hepatic focal lesions and 20 patients refused a liver biopsy. The remaining 155 G4-CHC patients completed all the study examinations and statistical analysis, and their datasets were available as shown in Fig. 1.

The study was approved by our institutional ethical committee and was conducted in accordance with the provisions of the Declaration of Helsinki. Written informed consent was obtained from participants before enrolment.

Clinical and diagnostic workup

At study entry, a thorough medical history and physical examination were taken for data collection: age, gender, body mass index (BMI), co-morbidities, and severity of the liver disease. Blood samples were collected for laboratory investigations included complete blood count, liver, and kidney function tests. The studied patients underwent abdominal ultrasonography to exclude hepatic focal lesions and for guiding non-targeted percutaneous liver biopsy. Both MDCT and MRI were done, and then, liver biopsy was done within a short time interval (less than 15 days) under local anesthesia according to standard procedures.

Imaging modalities

All the patients underwent MDCT and MRI examination of the liver in the radiology department at our institution. No iodinated or gadolinium-based contrast agents were used. The diagnosis was confirmed for all the patients by percutaneous liver biopsy.

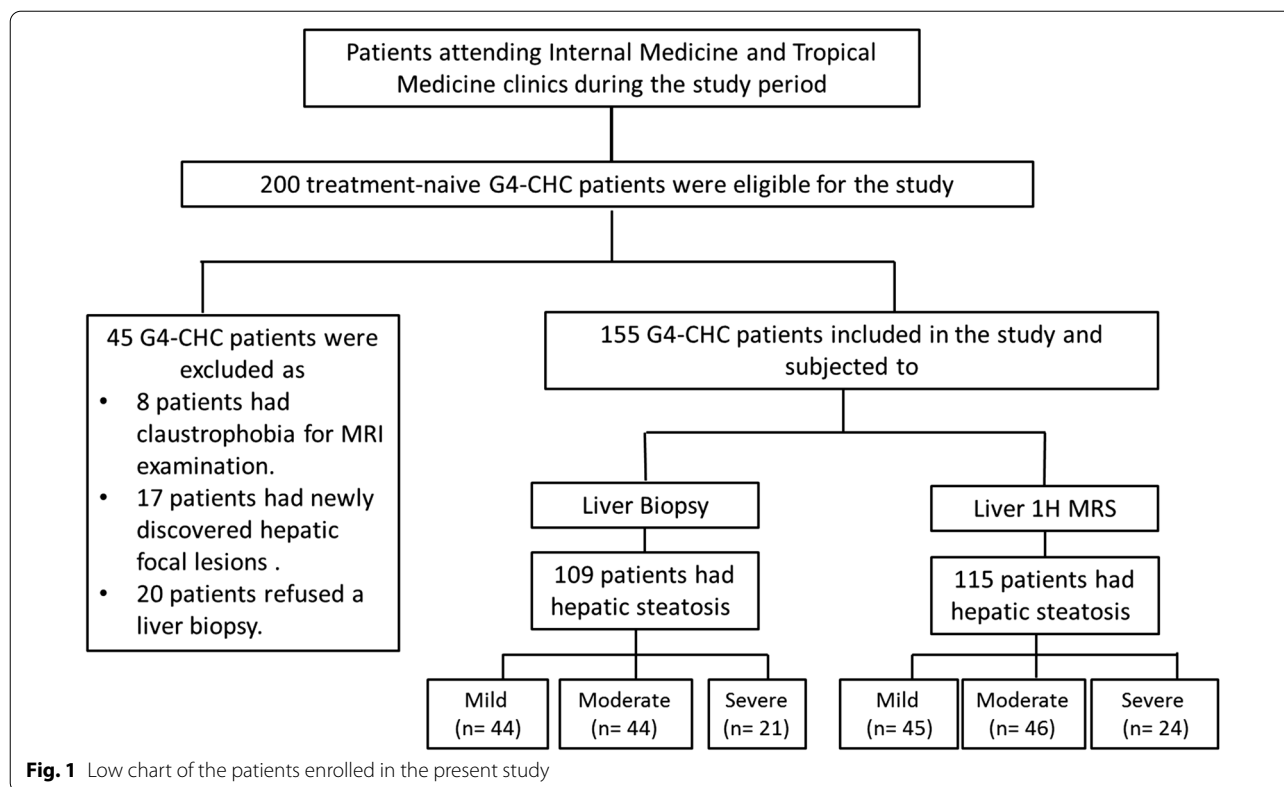
Technique

MDCT

All patients were examined in the supine position using 16 multidetector rows CT scanner (GE Lightspeed, GE Healthcare). No special preparation was needed. The non-contrast scan was obtained to cover the upper abdomen with the following parameters: 120 kV and 350 mAs, with 0.5 s rotation time and 1.375 pitch. Then, data were reconstructed at 2.5 mm slice thickness at 2.5-mm intervals.

MRI

All patients were examined in the supine position using a 1.5 T magnet (Achieva, Philips Healthcare, the Netherlands) and SENSE Torso XL coil. No special preparation was needed. A compression belt was used to reduce respiratory motion. The following sequences cover the upper abdomen: (1) axial T2-weighted turbo spin echo (T2W_TSE)((time to repetition [TR] 405 msc, time to echo [TE] 80 ms, flip angle 90°, matrix 256 × 162, field



of view [FOV] 375 mm, slice thickness 7 mm, gap 1 mm, number of signal average 1, scan time 13 s), (2) axial selective adiabatic inversion recovery (SPAIR); fat suppressed images (time to repetition [TR] 520msc, time to echo [TE] 80 ms, flip angle 90°, matrix 256 × 162, field of view [FOV] 375 mm, slice thickness 7 mm, gap 1 mm, number of signal average 1, scan time 13 s), (3) the dual-echo axial breath-hold T1-based gradient echo (GRE) imaging (in-phase/out-of-phase, IP/OP) routinely used for estimating liver fat (repetition time of 128 ms; echo time of 6.9 ms for OP images and 4.6 ms for IP images; flip angle, 80°; section thickness, 7 mm; matrix size, 192 × 188; FOV, 375 mm), (4) single-voxel proton (1H) MR spectroscopy (¹H-MRS) using point-resolved spectroscopy (PRESS) with long TR values after automatic shimming and it was acquired during free breathing. A localization voxel of 20 × 20 × 20 mm³ in the right hepatic lobe (V, VI, or VII segments) while avoiding large vessels, bile ducts, and liver edges (with a margin of 1–2 cm) in all three anatomic planes on the scout images. MRS data were obtained during single breath holding. The other scan parameters were as follows: TE, 30 ms; TR, 4000 ms; bandwidth, 1000 Hz; the number of acquisitions, two; water suppression, off; and acquisition time, 8 s, and (v) diffusion-weighted imaging (DWI), transverse echoplanar. Parallel imaging was performed with SENSE technology. Multiple breath-hold techniques were done,

each lasting 20 s, and were performed to cover the entire liver and the typical acquisition time was 80 s. *b* values of 0, 300, 600 s/mm² were used.

Analysis of images

Two radiologists with 18 and 10 years of experience in radiology revised the results of the MDCT and MRI blinded to the results of the liver histopathologic evaluation. All measurements were taken by both radiologists independently; then, one value was taken in consensus for each analysis.

1. Unenhanced CT, a qualitative estimation of liver fat is performed by comparing the attenuation of the liver with that of the spleen. For fat quantification, both hepatic attenuation measurement in Hounsfield units and calculation of the hepatic attenuation index using region-of-interest (ROI) measurement of hepatic and splenic attenuation. A liver-to-spleen attenuation ratio of ≤ 1.1 was used to assess hepatic steatosis [18].
2. Dual-echo T1-GRE imaging utilizes the difference in the resonance frequency of protons in water and protons in fat to detect and measure hepatic fat content by signal intensities measured in corresponding

regions of interest on IP and OP images. An internal reference (spleen) was used to correct the hepatic signal intensity values. The hepatic fat fraction is calculated by comparing the signal intensities on IP and OP images [19, 20].

$$\text{Fat signal fraction} = S_{\text{IP}} - s_{\text{OP}}/2S_{\text{IP}}$$

where S_{IP} is the net hepatic signal on IP images and S_{OP} is the net hepatic signal on OP images.

$$\text{Fat signal percentage} = 100 \times \text{liver } S_{\text{IP}}/\text{spleen } S_{\text{IP}} - \text{liver } S_{\text{OP}}/\text{spleen } S_{\text{OP}}/2 \times \text{liver } S_{\text{IP}}/\text{spleen } S_{\text{IP}}$$

where S_{IP} is the ratio of hepatic signal intensity to splenic signal intensity on IP images and S_{OP} is the ratio of hepatic signal intensity to splenic signal intensity on OP images.

3. Frequency-selective fat saturation

The fraction of relative signal intensity loss on the T2-weighted image without fat suppression (FS) and with a T2-weighted image with FS calculated as follows [21]

$$\text{fat percentage in liver (HFP)} = \text{nonFS} - \text{FS}/\text{nonFS} \times 100$$

4. Proton [^1H] MR spectroscopy (^1H -MRS)

Postprocessing of raw data from MRS was done using a vendor postprocessing package software. Manual phase adjustment was used, as well as the spectral shift of the display before integration. Lipid and water peak integral areas were obtained at set frequency limits and then corrected for relaxation. The total hepatic triglyceride content (TGC) is calculated by summing the individual lipid peaks in the 0.9–3.0 parts per million (ppm) region of the MR spectrum to obtain the total lipid peak area (TLPA). The sum of fat and water peaks calculated to obtain proton density fat fraction (PDFF) as follows [22]

$$\text{PDFF} = \text{fat signal peak area}(0.9 - 3\text{ppm})/\text{fat signal peak areas} + \text{water peak area}$$

However, the MRS spectra acquired in the left lobe in most of the subjects were corrupted by the artifact and not considered of sufficient quality to include in the analysis, and thus, measurements are most often only obtained in the right lobe.

Krššák et al. [14] yielded following staging—0: no steatosis resulting in less than 3.1% of MRS signal; stage 1: mild resulting in the range of 3.1–5.0% of MRS signal; stage 2: moderate resulting in the range of 5.0–6.9% of MRS signal; and stage 3: severe resulting in more than 6.9% of MRS signal.

5. DWI

The apparent diffusion coefficient (ADC) map was generated on a voxel-by-voxel basis by a commercially available software package (Philips MR workspace, Philips Medical System; Eindhoven, the Netherlands). Regions of interest of 2 cm² were placed in each segment of the right lobe avoiding areas of artifact or vessels. The left lobe segments were excluded from our measurements due to the possible cardiac motion artifacts. The mean ADC value was calcu-

lated for each case to infer hepatic fibrosis.

Liver biopsy and histopathological analysis

For histological analysis, the samples were routinely processed, formalin-fixed and paraffin-embedded, stained with hematoxylin/eosin for steatosis and inflammation, and Masson's trichrome stain for assessment of fibrosis. The histopathologic grades provided by the pathologist according to the nonalcoholic steatohepatitis (NASH) Clinical Research Network Scoring System definitions [23]. Steatosis, ballooning, lobular inflammation, and fibrosis were staged: steatosis involving <5% of cells (S0, no steatosis), 5–33% (S1, mild), >33–66% (S2, moderate), and >66% (S3, severe) of hepatocytes. Ballooning was graded as none (0), few balloon cells (1), and many cells/prominent ballooning (2). Lobular inflammation was graded as no foci (0, none), <2 foci (1, mild), 2–4 foci (2, moderate), and >4 foci per 200 × field (3, marked). Fibrosis was staged as none (F0), portal fibrosis: fibrous portal expansion (F1), periportal fibrosis (F2), bridging fibrosis, and distorted architecture (F3), and cirrhosis (F4). The diagnosis of non-alcoholic fatty liver disease (NAFLD) was made if steatosis was ≥5% and either ballooning or lobular inflammation or both were absent. The diagno-

sis of NASH was made when steatosis was ≥5% and ballooning and lobular inflammation were present [24].

Statistical analysis

All statistical analyses were carried out using SPSS for Windows version 16 (IBM Corp., Armonk, NY, USA) and the MedCalc program. Inter-rater agreement for each test was calculated using Cohen's kappa coefficient (j) which is calculated as follows: $j = (p_0 - p_e)/(1 - p_e)$, where p_0 is the observed proportion of agreement and p_e is the expected proportion of agreement. Quantitative data are expressed as mean ± standard deviation or median

and the range for normally or abnormally distributed data and qualitative data were expressed as a percentage. Spearman's rank correlation coefficient (r) was used to find correlations. The receiver operating characteristic (ROC) curves were plotted to measure and compare the performance of different noninvasive imaging parameters in predicting hepatic steatosis and its grades. The best cutoff values were chosen to calculate sensitivity, specificity, positive (PPV) and negative (NPV) predictive value, positive and negative likelihood ratio (+LR, -LR) for predicting hepatic steatosis. All tests were two-tailed and statistical significance was assessed at <0.05 .

Results

Characteristics of the study patients

The mean age of the total 155 patients was 43.2 ± 12.9 years and the majority of them were males (119/155, 76.8%). Their mean BMI was 25.6 ± 2.9 kg/m² where, more than half of the cases were overweight ≥ 25 kg/m² (87/155, 56.6%). Further clinical and

laboratory characteristics of the studied patients are summarized in Table 1

Histologically, hepatic steatosis was found in 109 (70.3%) of 155 CHC patients. The degree of hepatic steatosis was mild in 44, moderate in 44, and severe in 21 cases. Furthermore, staging for liver fibrosis showed different stages (F1: $n = 54$, F2: $n = 62$, F3: $n = 13$, F4: $n = 26$).

Characteristics of imaging modalities and their correlation with histopathological data

We found that 78 cases (50.3%) had a low CT ratio (≤ 1.1). We found no correlation between the CT ratio and pathological grading of hepatic steatosis ($r = -0.090$, $p = 0.614$).

As regarding MRI modalities, T1-fat fraction ranged between (-32.5 to 30.4%) throughout the liver with the median of -13.5% and 3.2% for the voxel placed in the anterior part of the right liver lobe. Furthermore, the median total proton density fat fraction was 12.5%

Table 1 Demographic and clinical characteristics of the study patients with genotype-4 chronic hepatitis C

Variables	Number of patients = 115
Age (years, mean \pm SD & range)	43.2 \pm 12.9 (21–62)
Sex (male/female)	119/36 (76.8/23.2%)
BMI (kg/m ² , mean \pm SD)	25.6 \pm 2.9
Average weight (BMI < 25)	68 (43.9%)
Overweight (BMI 25–30)	87 (56.1%)
Obese (BMI > 30)	0
Serum albumin (g/dL, mean \pm SD)	3.8 \pm 0.7
Serum bilirubin (mg/dL, median & range)	1.4 (0.6–5.8)
ALT (U/L, mean \pm SD)	41.5 \pm 20.3
AST (U/L, mean \pm SD)	38.9 \pm 18.3
ALP (U/L, mean \pm SD)	119.4 \pm 48.7
Platelet count (10 ³ / μ L, U/L, mean \pm SD)	201.7 \pm 72.2
HCV RNA (IU/mL, median & range)	4.5 $\times 10^5$ (9 $\times 10^3$ –8 $\times 10^6$)
<i>Histopathological data</i>	
Fibrosis stage (F1/F2/F3/F4)	54/62/13/26 (34.8/40/8.4/16.8)
Hepatitis grades (G1/G2/G3)	68/58/29 (43.9/37.4/18.7)
Steatosis (no/mild/moderate/severe)	23/44/44/21 (29.7/28.4/28.4/13.5)
<i>MDCT data</i>	
CT ratio (mean \pm SD, range)	1.1 \pm 0.2 (0.3–1.4)
<i>MRI data</i>	
T1-fat fraction (median & range)	-13.5 (-32.5 to 30.4)
Fat percentage (median & range)	4.8 (-5.2 to 33.4)
T2 fat suppression (median & range)	0.1 (-22.5 to 22.2)
Proton density fat fraction% (PDFF) (median & range)	6.2 (0.6–35.2)
ADC for hepatic fibrosis ($\times 10^{-3}$ mm ² /s) (median & range)	1.2 (0.97–1.4)

ADC apparent diffusion coefficient, ALT alanine aminotransferase, ALP alkaline phosphatase, AST aspartate aminotransferase, BMI body mass index, SD standard deviation, MDCT multidetector computed tomography, MRI magnetic resonance imaging

(1.26–70.43%) throughout the right lobe of the liver providing a wide range of liver fat content (Table 1).

We found that proton density fat fraction was significantly correlated with the histopathologic staging of fibrosis ($r=0.707$, $p\leq 0.001$), grading of steatosis ($r=0.953$, $p<0.001$), and grading of hepatitis (lobular inflammation) ($r=0.791$, $p<0.001$) and negatively correlated with ADC for hepatic fibrosis ($r=-0.476$ and $p=0.004$), while the T1-fat fraction and fat percentage were correlated with steatosis grading ($r=0.380$, $p=0.027$ and $r=0.384$, $p=0.025$, respectively) as shown in Fig. 2. On the other hand, no correlation was found between fat suppression and steatosis grades ($r=0.088$, $p=0.620$).

In addition, no correlations were found between age, gender, BMI and liver enzymes (ALT and AST), serum virological load and histological stages of steatosis, or the evaluated liver fat metrics of CT, and MRI ($p>0.05$).

Diagnostic performance of MDCT and MRI parameters for prediction of hepatic steatosis

Based on the ROC curves, T1-fat fraction, Fat percentage and proton density fat fraction had good prognostic accuracy for the prediction of hepatic steatosis where proton density fat fraction yielded the highest AUC (0.958) and 95% confidence interval (CI) (0.828–0.995, $p<0.001$), with 95.8% sensitivity and 90% specificity at a cutoff of >4.95 followed by T1-fat fraction (0.808) and fat percentage (0.702) as shown in (Table 2; Fig. 3a).

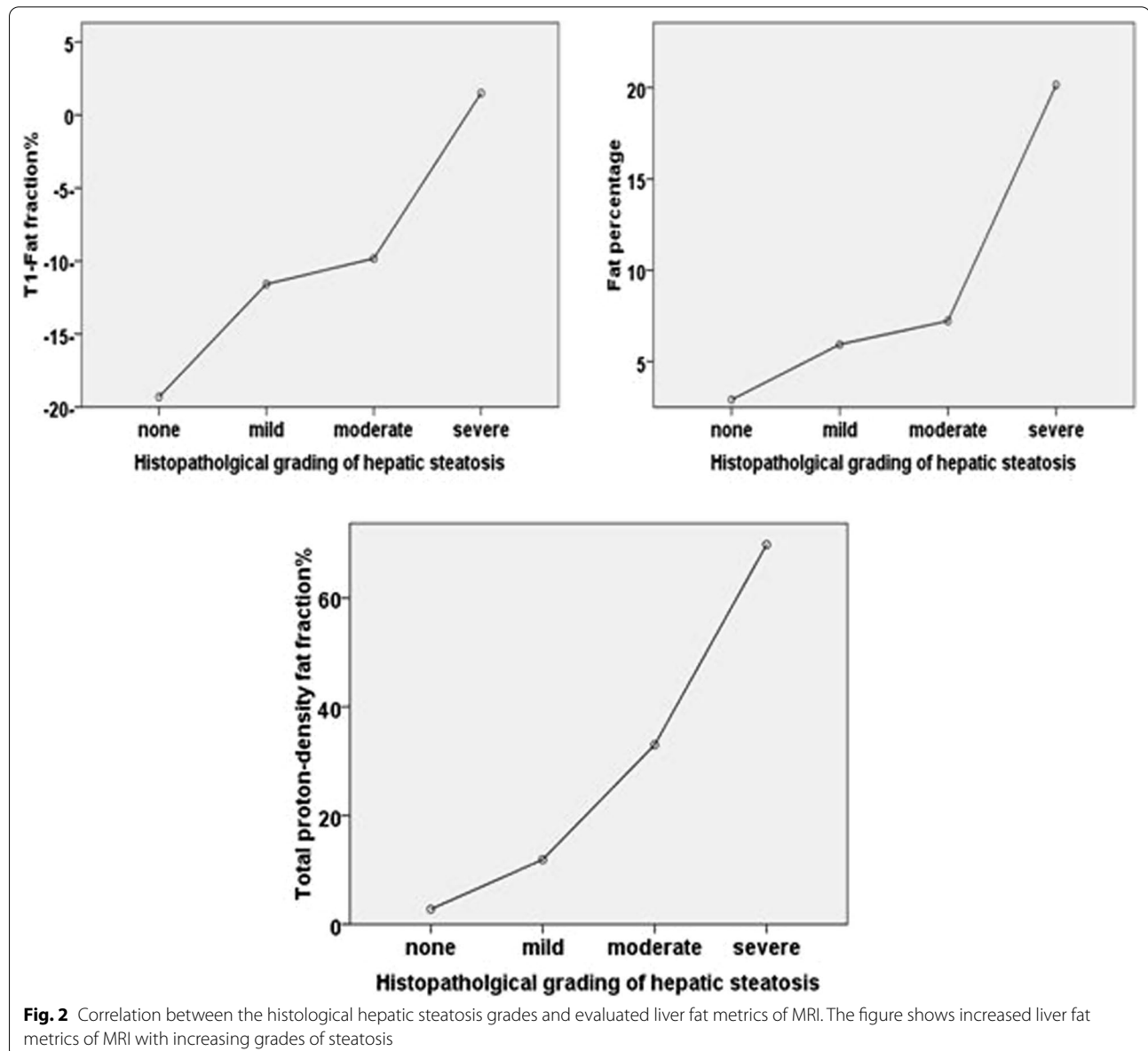


Table 2 Diagnostic accuracy of magnetic resonance imaging (MRI) parameters to predict hepatic steatosis with the best predictive cutoffs

	AUC (95% CI)	SE	SP	PPV	NPV	+LR	–LR	<i>p</i>
<i>For the prediction of liver steatosis</i>								
T1-fat fraction > -13.7%	0.808 (0.637–0.922)	66.7	90	94	53.5	6.7	0.4	<0.001
Fat percentage (> 5.1%)	0.702 (0.521–0.846)	54.2	80	86.4	42.7	2.7	0.6	0.030
Proton density fat fraction (> 4.95%)	0.958 (0.828–0.995)	95.8	90	95.7	90.1	9.6	0.1	<0.001
<i>For the prediction of mild liver steatosis</i>								
T1-fat fraction > -13.7%	0.845 (0.622–0.963)	72.7	90	74.4	89.2	7.3	0.3	<0.001
Fat percentage (> 5.1%)	0.650 (0.414–0.841)	45.5	80	47.7	78.6	2.3	0.7	0.217
Proton density fat fraction (> 4.95%)	0.910 (0.701–0.987)	91	90	78.5	96.1	9.1	0.1	<0.001
<i>For the prediction of moderate liver steatosis</i>								
T1-fat fraction (> 0.4%)	0.654 (0.466–0.812)	27.3	100	100	77.4	–	0.7	0.147
Fat percentage (> 2.8%)	0.652 (0.463–0.810)	90.9	38.1	37	91.3	1.5	0.2	0.154
Proton density fat fraction (> 8.44%)	0.931 (0.782–0.988)	100	85.7	73.7	100	7	0	<0.001
<i>For the prediction of severe liver steatosis</i>								
T1-fat fraction (> 6.2%)	0.619 (0.445–0.773)	40	100	100	91.8	–	0.6	0.942
Fat percentage (> 6.1%)	0.850 (0.694–0.945)	100	65.6	30.3	100	2.9	0	0.0742
Proton density fat fraction (> 20.4%)	0.975 (0.861–0.995)	100	93.8	70.7	100	16	0	<0.001

AUC area under the receiver operating characteristic curve, +LR positive likelihood ratio, –LR negative likelihood ratio, NPV negative predictive value, PPV positive predictive value, SP specificity, SE sensitivity

The ROC curves evaluated the diagnostic accuracies of these MRI parameters to determine which parameter would have the most clinical utility to predict different stages of liver steatosis as defined by histological stages. For predicting mild steatosis (Fig. 3b), the AUC was greatest for the total proton density fat fraction (0.910) followed by T1-fat fraction (0.845), then the fat percentage (0.650). For predicting moderate steatosis (Fig. 3c), the AUC was greatest for the total proton density fat fraction (0.931), followed by the T1-fat fraction (0.654) and fat percentage (0.652). To predict severe steatosis (Fig. 3d), the AUC was greatest for total proton density fat fraction (0.975) followed by fat percentage (0.850) then T1-fat fraction (0.619).

In addition, using the ROC curves, we calculated the cutoff values of the total proton density fat fraction to discriminate different steatosis grades (Table 2). With a cutoff value > 4.95%, total fat fraction% had 91% sensitivity, 90% specificity, 78.5% PPV, and 96.1% NPV for the prediction of mild steatosis. At a cutoff value > 8.4, total fat fraction% had 100% sensitivity, 85.7% specificity, 73.7% PPV, and 100% NPV for the prediction of moderate steatosis. Furthermore, at a cutoff value > 20.4% total fat fraction% had 100% sensitivity, 93.8% specificity, 70.7% PPV, and 100% NPV for the prediction of severe steatosis.

On comparison of steatosis grading by histology and ¹H-MRS, we found an agreement between these methods in 74.2% of patients as shown in (Table 3) with the highest percentage of correct diagnosis in mild steatosis (75%) and the lowest percentage of correct diagnosis in

moderate steatosis (65.9%). The distribution of steatosis grading by histology and ¹H-MRS in different fibrosis stages was shown in (Table 4) (Figs. 4, 5).

Interobserver reproducibility of MDCT and MRI in quantitative assessment of hepatic steatosis

As regards the interrater agreement in this study, there was substantial agreement in the qualitative estimation of liver fat in non-enhanced MDCT examinations (0.78), and almost perfect agreement in quantitative fat assessment in MDCT, dual-echo T1-GRE imaging, frequency-selective fat saturation, proton [1H] MR spectroscopy, and ADC measurements (0.85–0.97) between the two readers.

Discussion

This prospective study showed the diagnostic performance of liver fat metrics of MRI as noninvasive methods for the detection of hepatic steatosis in Egyptian G4-CHC patients. Elaborating reliable models to predict liver steatosis in those patients remains a challenge for hepatologists. Identification of significant steatosis (moderate and severe) is an important parameter for antiviral treatment.

Out of the 155 patients included in our study, 109 patients (70.3%) showed evidence of steatosis on histopathological examination of liver biopsies that were

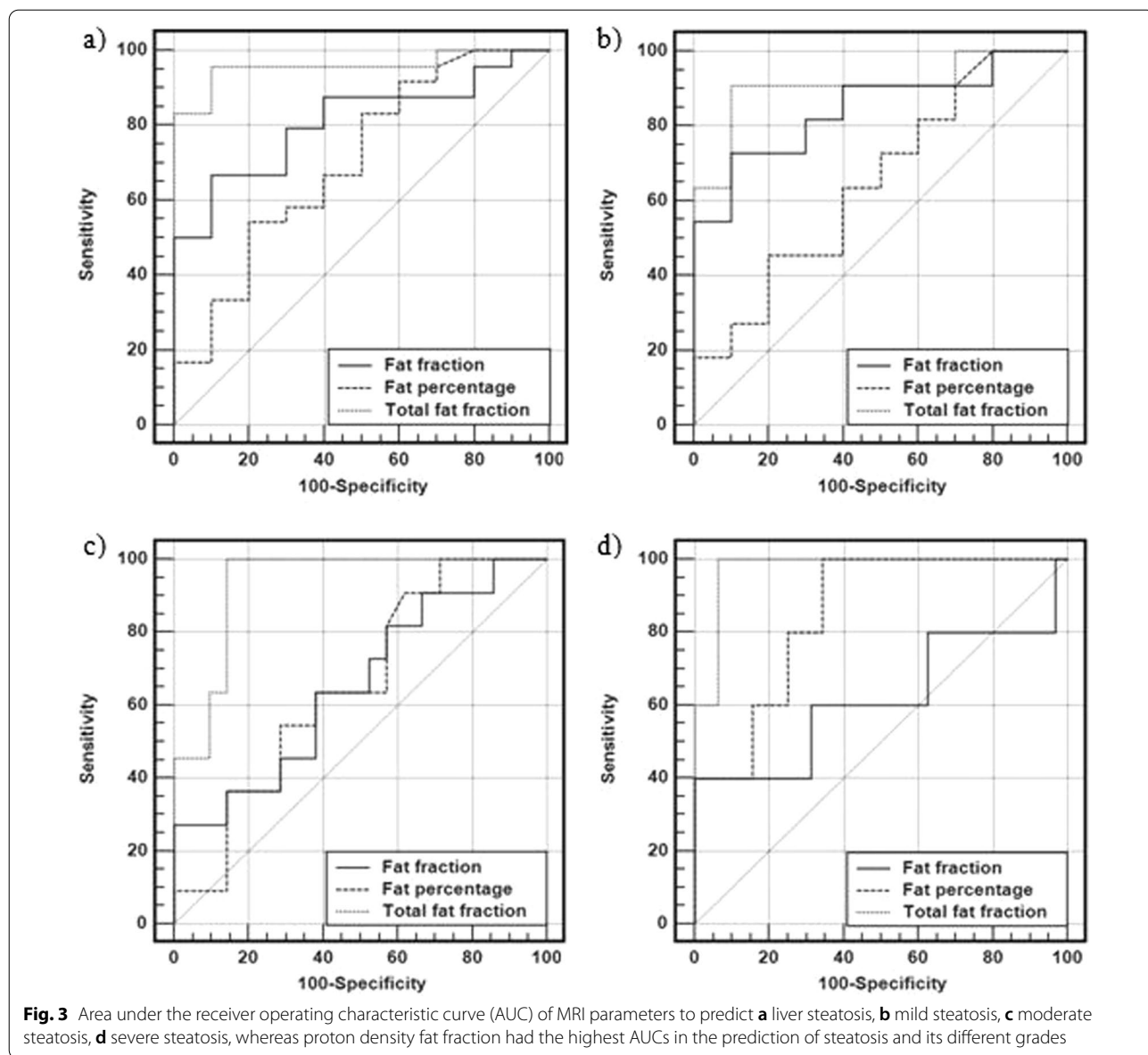


Fig. 3 Area under the receiver operating characteristic curve (AUC) of MRI parameters to predict **a** liver steatosis, **b** mild steatosis, **c** moderate steatosis, **d** severe steatosis, whereas proton density fat fraction had the highest AUCs in the prediction of steatosis and its different grades

Table 3 Comparison between hepatic steatosis staging by histology and 1H MRS

Liver steatosis grades by histology ^a	Liver steatosis grades by 1H MRS ^a			
	No (n = 40)	Mild (n = 45)	Moderate (n = 46)	Severe (n = 24)
None (n = 46)	36	6	4	0
Mild (n = 44)	4	33	7	0
Moderate (n = 44)	0	6	29	9
Severe (n = 21)	0	0	6	15

^a Cutoff values for hepatic steatosis were 5, 33, and 66% of involved hepatocytes for histology and 4.95, 8.4, and 20.3% of MRS signal for 1H MRS method. In 74% of patients an agreement between

histological and 1H MRS steatosis assessment was achieved

within the range of previous studies [25, 26] showing that hepatic steatosis is a feature of G4-HCV infection.

Consistent with earlier studies [27–30], we found liver fat metrics of ¹H-MRS correlated with the histological grading of hepatic steatosis in CHC patients. Kršák et al.[14] stated that a significant correlation between ¹H-MRS and histological steatosis was further confirmed by biochemical analysis of extracted tissue samples.

In this study, liver fat metrics of ¹H-MRS had the potential to predict hepatic steatosis, whereas the diagnostic accuracy of MRS total proton density fat fraction with an AUC of 0.958, 95.8% sensitivity, 90% specificity, 95.7% PPV, and 90.1% NPV at a cutoff > 4.95%. Our

Table 4 Distribution of hepatic steatosis grade as assessed by histology /MRS in different fibrosis stages

Liver fibrosis stages	Liver steatosis grades by histology/MRS			
	No (n = 46/40)	Mild (n = 44/45)	Moderate (n = 44/46)	Severe (n = 21/24)
F1 (N= 54)	46/36	6/18	2/0	0
F2 (N=62)	0/4	38/27	24/31	0
F3 (N= 13)	0/0	0/0	4/10	9/3
F4 (N= 26)	0	0	14/5	12/21

results were supported by Rastogi et al. [27] who demonstrated that MRS had an AUC of 0.959 with 94% sensitivity, 97% specificity, 95% NPV, and 96% accuracy to diagnose liver steatosis at a cutoff value of 6.27.

We found that the total proton density fat fraction showed the best diagnostic performance for predicting different grades of steatosis (AUC=0.910, 0.931, and 0.975 for mild, moderate, and severe steatosis, respectively) compared to the other MRI metrics; fat fraction

and percentage. Moreover, at cutoff >4.95, ¹H-MRS can discriminate mild steatosis from no steatosis (91% sensitivity, 90% specificity, 78.5% PPV and 96.1% NPV). It can predict moderate steatosis (100% sensitivity, 85.7% specificity, 73.7% PPV and 100% NPV) with a cutoff value >8.4. Additionally, it can predict severe steatosis with a cutoff value >20.4 (100% sensitivity, 93.8% specificity, 70.7% PPV, and 100% NPV). Krššák et al. [14] assessed grades of hepatic steatosis based on ¹H-MRS results using different

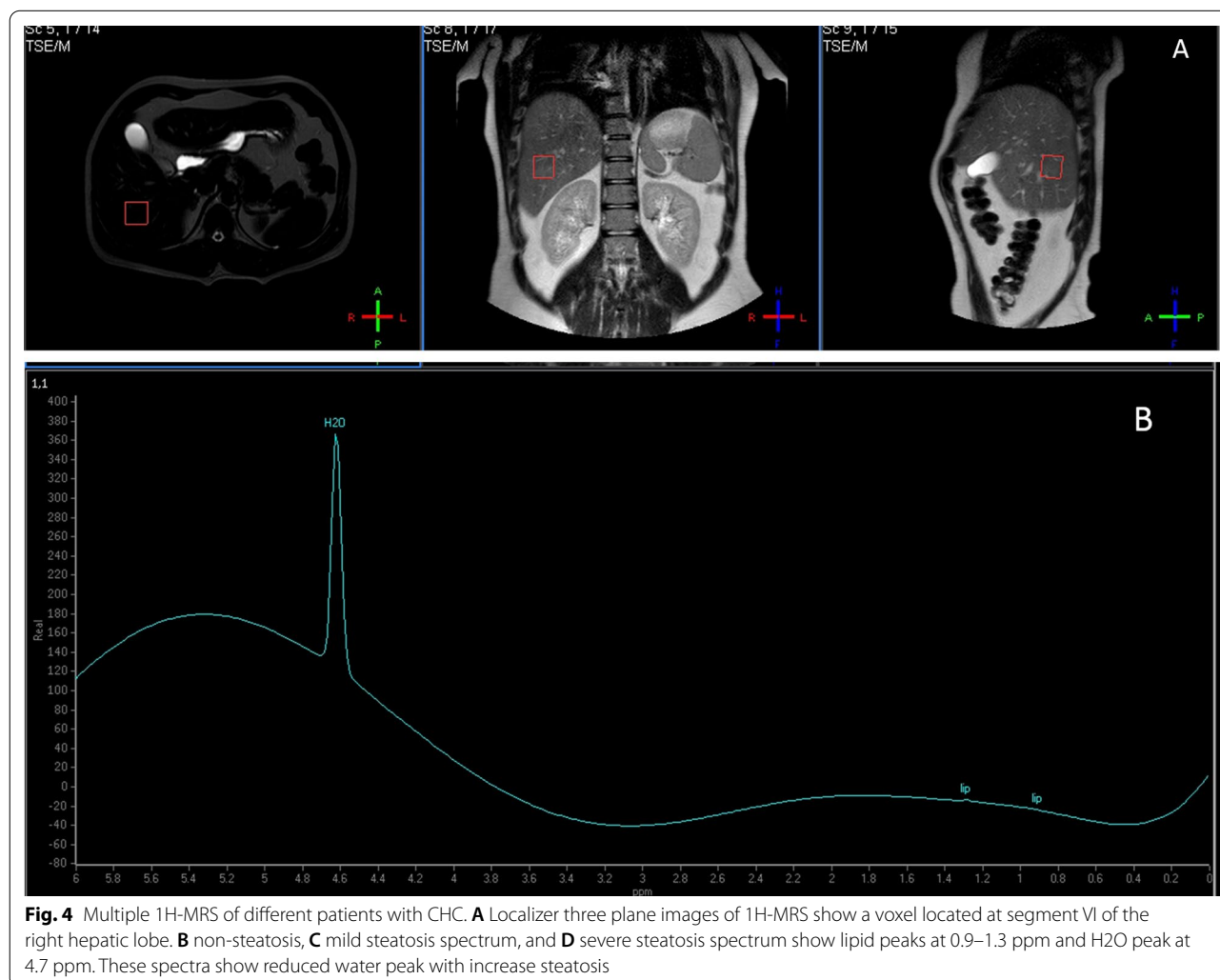


Fig. 4 Multiple 1H-MRS of different patients with CHC. **A** Localizer three plane images of 1H-MRS show a voxel located at segment VI of the right hepatic lobe. **B** non-steatosis, **C** mild steatosis spectrum, and **D** severe steatosis spectrum show lipid peaks at 0.9–1.3 ppm and H2O peak at 4.7 ppm. These spectra show reduced water peak with increase steatosis

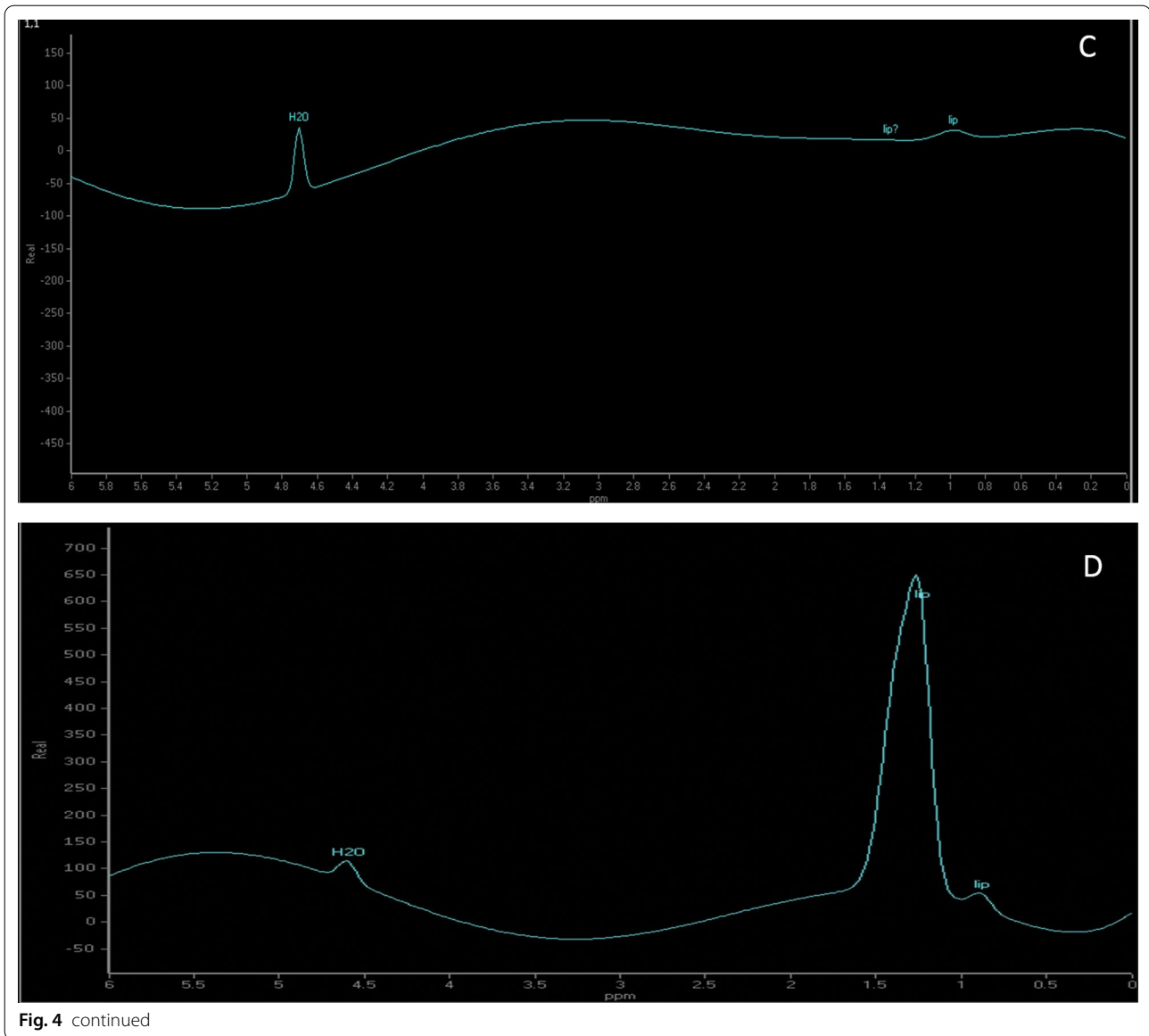


Fig. 4 continued

cutoff values; <3.1%, 3.1–5.0%, 5.0–6.9%, and >6.9% for no, mild, moderate, and severe steatosis, respectively. The high cutoff values for the diagnosis of significant steatosis (moderate and severe) in our study may be attributed to the presence of hepatic fibrosis affecting the imaging of steatosis.

Noureddin et al. [31] reported that ¹H-MRS was a reliable noninvasive method to evaluate the whole liver parenchyma including a complete assessment of liver fat content (FC). This is particularly relevant in patients with heterogeneous hepatic steatosis in which sensitivity of liver biopsy is limited as less than 1/50,000th of the liver is available for histopathological examination [32].

The current study showed no correlation between the CT ratio and histopathological grading of hepatic

steatosis. Contrary to our finding, Rastogi, et al. [27] reported that CT fat quantification correlated well with liver biopsy results ($r=0.715$); however, it was inferior to MR methods for liver fat estimation. It has further limitations in providing semiquantitative nature of findings rather than discrete values for fat content. The poor performance of the CT ratio in detecting steatosis might be due to the small number of CHC patients included in this study.

In this study, we found that hepatic fat content measured by proton density fat fraction correlated with lobular inflammation. These findings were consistent with previous studies indicating an influence of steatosis on the necroinflammatory activity of HCV [33, 34].

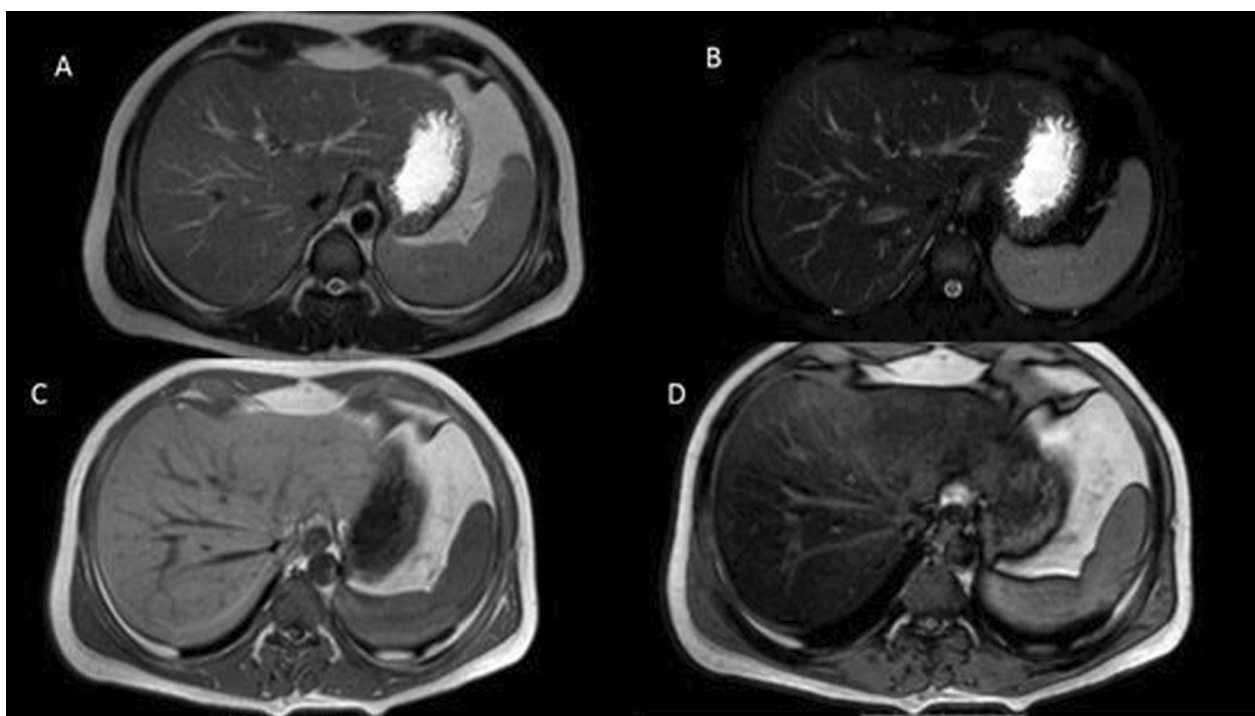


Fig. 5 A 30-year-old male patient with CHC **A** axial T2WI, **B** axial SPIR, **C** axial T1-in-phase, **D** T1-out-of-phase. **A, B** Signal intensity of the liver drops compared to spleen because the fat-saturated pulse suppresses the signal from fat within the liver. **C, D** Marked signal dropout on out-of-phase imaging indicating the presence of diffuse steatosis with calculated fat fraction and fat percentage about 30.40 and 33.44, respectively, indicating severe steatosis

In CHC, precise mechanisms leading to hepatic steatosis are complex and not well characterized, e.g., oxidative stress, cytokine release, inflammation, insulin resistance, and impaired lipid and carbohydrate metabolism may initiate the development of steatosis, worse fibrosis, and reduce therapeutic response. Steatosis in hepatitis C appears to be genotype-specific [35]. It is predominantly cytopathic in genotype 3 (G3) in which a sustained virological response is associated with hepatic steatosis reduction [15] and metabolic in non-G3 hepatitis C that may reduce the success of antiviral therapy [36]. Regarding genotype 4, hepatic steatosis was mostly associated with metabolic factors, similar to those in genotype 1; however, the possibility of the presence of viral-induced steatosis was also accused [37, 38].

Fishbein et al. [39] showed that hepatic MRI, based upon chemical shift imaging, was able to accurately quantify the hepatic FC even in patients with significant hepatic fibrosis. Concomitantly, in our study, ^1H -MRS; total proton density fat fraction, could assess hepatic steatosis in 76.6% of CHC patients with hepatic fibrosis. In line with previous studies [40, 41], we reported a significant correlation between quantification of hepatic FC based on total proton density fat fraction and hepatic fibrosis (diagnosed histologically

and by ADC) in CHC patients. These findings were matched with previous studies. Moreover, Kršák et al. [14] and Orlacchio et al. [28] revealed uniform distribution of steatosis grades across all fibrosis stage groups indicating that hepatic steatosis may accelerate liver fibrosis. Hepatic steatosis may induce fibrosis through insulin resistance and oxidative stress leading to lipid peroxidation and cytokine release [8]. Also, prolonged lipid storage can result in inflammatory reactions and loss of metabolic competence [42]. Modaresi Esfeh and Ansari-Gilani [43] revealed that steatosis in CHC patients was associated with more severe histological injury and higher fibrosis scores, suggesting that fat in the liver is biologically active tissue. Unlike our findings, Cho et al. [44] reported that an increased hepatic metabolite/fat ratio, as assessed by localized ^1H -MRS, correlated with fibrosis staging suggesting decreased steatosis in higher fibrosis stages.

Although this study is one of the few studies which investigated liver fat metrics of CT and MRI in G4-CHC patients with hepatic fibrosis, it has some limitations. This series was a small-sized sample and a single-center study, so, the sample may not exactly represent the general population of CHC patients. Hence, further multicenter studies with larger populations are needed to confirm these

results, validate their usefulness in clinical practice, and assess the dynamic changes in liver fat metrics of MRI during antiviral therapy. Although the principle of MRS to quantify hepatic steatosis is straightforward, there were some biases in its acquisition, e.g., T1 and T2 relaxation effects were well-known biases of MRS to evaluate hepatic steatosis in addition to the presence of excessive iron. In addition, MDCT, however, had a limited diagnostic accuracy for detecting mild hepatic steatosis in addition to potential hazard of radiation exposure.

Conclusions

¹H-MRS had a good diagnostic performance in diagnosis and quantification of hepatic steatosis whereas ¹H-MRS; a proton density fat fraction has the highest diagnostic accuracy as a noninvasive quantitative modality for hepatic steatosis and its different grades that may influence the course of chronic HCV infection and possibly its response to the antiviral therapy. It may have important clinical applicability, especially in those liver biopsies, which cannot be done.

Abbreviations

MDCT: Multidetector computed tomography; MRI: Magnetic resonance imaging; G4-CHC: Genotype 4-chronic hepatitis C; CHC: Chronic hepatitis C; ¹H-MRS: Proton magnetic resonance spectroscopy; AUC: Area under curve; NAFLD: Non-alcoholic fatty liver disease; HIV: Human immunodeficiency virus; CV: Hepatitis C virus; CL: Hepatocellular lipid content; ALT: Alanine transaminase; AST: Aspartate transaminase; RNA: Ribonucleic acid; HBV: Hepatitis B virus; BMI: Body mass index; TSE: Turbo spin echo; TR: Time to repetition; TE: Time to echo; FOV: Field of view; SPAIR: Selective adiabatic inversion recovery; GRE: Gradient echo; IP: In-phase; OP: Out-of-phase; PRESS: Point-resolved spectroscopy; DWI: Diffusion weighted imaging 4; ROI: Region of interest; S_{OP} : The net hepatic signal on OP images; S_{IP} : Net hepatic signal on IP images; FS: Fat suppression; HFP: Fat percentage in liver; TGC: Total hepatic triglyceride content; TSPA: Total lipid peak area; PDFF: Proton density fat fraction; ADC: Apparent diffusion coefficient; NASH: Non-alcoholic steatohepatitis; FC: Fat content.

Acknowledgements

Not applicable.

Authors' contributions

GSS designed the study, collected and analyzed the data, and drafted and revised the manuscript. EAH and HMI designed the study, recruited the patients, collected the data and revised the manuscript. RM interpreted the pathological data. NKI and MAG did laboratory work and interpreted the data. RME designed the study, interpreted the data, drafted and revised the manuscript, and managed the publication. All authors have read and approved the manuscript.

Funding

This research did not receive any specific grant from funding agencies in the public, commercial, or not-for-profit sectors.

Availability of data and materials

The datasets used and/or analyzed during the current study are available on reasonable request.

Declarations

Ethics approval and consent to participate

This study has been approved by the ethical committee of the Faculty of Medicine, Assiut University. The approval number is not applicable. A written consent was obtained from each study participant.

Consent for publication

Not applicable.

Competing interests

The authors declare that they have no competing interests.

Author details

¹Present Address: Department of Radiology, Faculty of Medicine, Assiut University, Assiut, Egypt. ²Department of Gastroenterology and Tropical Medicine, Assiut University, Assiut, Egypt. ³Department of Internal Medicine, Assiut University, Assiut, Egypt. ⁴Department of Pathology, Assiut University, Assiut, Egypt. ⁵Department of Biochemistry, Assiut University, Assiut, Egypt. ⁶Department of Radiology and Medical imaging, College of Medicine, Taibah University, Madinah, Saudi Arabia.

Received: 17 March 2021 Accepted: 15 August 2021

Published online: 24 August 2021

References

- Persico M, Iolascon A (2010) Steatosis as a co-factor in chronic liver diseases. *World J Gastroenterol* 16(10):1171–1176. <https://doi.org/10.3748/wjg.v16.i10.1171>
- Reeder SB, Sirlin CB (2010) Quantification of liver fat with magnetic resonance imaging. *Magn Reson Imaging Clin N Am* 18(3):337–ix. <https://doi.org/10.1016/j.mric.2010.08.013>
- Angulo P, Keach JC, Batts KP, Lindor KD (1999) Independent predictors of liver fibrosis in patients with nonalcoholic steatohepatitis. *Hepatology* (Baltimore, MD) 30(6):1356–1362. <https://doi.org/10.1002/hep.510300604>
- Gramlich T, Kleiner DE, McCullough AJ, Matteoni CA, Boparai N, Younossi ZM (2004) Pathologic features associated with fibrosis in nonalcoholic fatty liver disease. *Hum Pathol* 35(2):196–199. <https://doi.org/10.1016/j.humpath.2003.09.018>
- Ekstedt M, Franzén LE, Mathiesen UL, Thorelius L, Holmqvist M, Bodemar G, Kechagias S (2006) Long-term follow-up of patients with NAFLD and elevated liver enzymes. *Hepatology* (Baltimore, MD) 44(4):865–873. <https://doi.org/10.1002/hep.21327>
- Bach N, Thung SN, Schaffner F (1992) The histological features of chronic hepatitis C and autoimmune chronic hepatitis: a comparative analysis. *Hepatology* (Baltimore, MD) 15(4):572–577. <https://doi.org/10.1002/hep.1840150403>
- Czaja AJ, Carpenter HA (1993) Sensitivity, specificity, and predictability of biopsy interpretations in chronic hepatitis. *Gastroenterology* 105(6):1824–1832. [https://doi.org/10.1016/0016-5085\(93\)91081-r](https://doi.org/10.1016/0016-5085(93)91081-r)
- Lonardo A, Adinolfi LE, Loria P, Carulli N, Ruggiero G, Day CP (2004) Steatosis and hepatitis C virus: mechanisms and significance for hepatic and extrahepatic disease. *Gastroenterology* 126(2):586–597. <https://doi.org/10.1053/j.gastro.2003.11.020>
- Noureddin M, Wong MM, Todo T, Lu SC, Sanyal AJ, Mena EA (2018) Fatty liver in hepatitis C patients post-sustained virological response with direct-acting antivirals. *World J Gastroenterol* 24(11):1269–1277. <https://doi.org/10.3748/wjg.v24.i11.1269>
- Lok AS, Everhart JE, Chung RT, Kim HY, Everson GT, Hoefs JC, Greenon JK, Sterling RK, Lindsay KL, Lee WM, Di Bisceglie AM, Bonkovsky HL, Ghany MG, Morishima C, HALT-C Trial Group (2009) Evolution of hepatic steatosis in patients with advanced hepatitis C: results from the hepatitis C antiviral long-term treatment against cirrhosis (HALT-C) trial. *Hepatology* (Baltimore, MD) 49(6):1828–1837. <https://doi.org/10.1002/hep.22865>
- Lok AS, Everhart JE, Chung RT, Padmanabhan L, Greenon JK, Shiffman ML, Everson GT, Lindsay KL, Bonkovsky HL, Di Bisceglie AM, Lee WM, Morgan TR, Ghany MG, Morishima C, HALT-C Trial Group (2007) Hepatic steatosis in hepatitis C: comparison of diabetic and nondiabetic patients

- in the hepatitis C antiviral long-term treatment against cirrhosis trial. *Clin Gastroenterol Hepatol* 5(2):245–254. <https://doi.org/10.1016/j.cgh.2006.11.002>
12. Cheng FK, Torres DM, Harrison SA (2014) Hepatitis C and lipid metabolism, hepatic steatosis, and NAFLD: still important in the era of direct acting antiviral therapy? *J Viral Hepatitis* 21(1):1–8. <https://doi.org/10.1111/jvh.12172>
 13. Lonardo A, Adinolfi LE, Restivo L, Ballestri S, Romagnoli D, Baldelli E, Nascimbeni F, Loria P (2014) Pathogenesis and significance of hepatitis C virus steatosis: an update on survival strategy of a successful pathogen. *World J Gastroenterol* 20(23):7089–7103. <https://doi.org/10.3748/wjg.v20.i23.7089>
 14. Krssák M, Hofer H, Wrba F, Meyerspeer M, Brehm A, Lohninger A, Steindl-Munda P, Moser E, Ferenci P, Roden M (2010) Non-invasive assessment of hepatic fat accumulation in chronic hepatitis C by 1H magnetic resonance spectroscopy. *Eur J Radiol* 74(3):e60–e66. <https://doi.org/10.1016/j.ejrad.2009.03.062>
 15. Hofer H, Bankl HC, Wrba F, Steindl-Munda P, Peck-Radosavljevic M, Osterreicher C, Mueller C, Gangl A, Ferenci P (2002) Hepatocellular fat accumulation and low serum cholesterol in patients infected with HCV-3a. *Am J Gastroenterol* 97(11):2880–2885. <https://doi.org/10.1111/j.1572-0241.2002.07056.x>
 16. Kouyoumjian SP, Chemaitelly H, Abu-Raddad LJ (2018) Characterizing hepatitis C virus epidemiology in Egypt: systematic reviews, meta-analyses, and meta-regressions. *Sci Rep* 8(1):1661. <https://doi.org/10.1038/s41598-017-17936-4>
 17. Anwar W, Sarwar M, Hussain AB, Tariq WU, Saif M (2006) Significance of occult HBV infection in patients with chronic hepatitis C. *J Coll Phys Surg-Pak* 16(3):192–195
 18. Boyce CJ, Pickhardt PJ, Kim DH, Taylor AJ, Winter TC, Bruce RJ, Lindstrom MJ, Hinshaw JL (2010) Hepatic steatosis (fatty liver disease) in asymptomatic adults identified by unenhanced low-dose CT. *AJR Am J Roentgenol* 194(3):623–628. <https://doi.org/10.2214/AJR.09.2590>
 19. Qayyum A, Goh JS, Kakar S, Yeh BM, Merriman RB, Coakley FV (2005) Accuracy of liver fat quantification at MR imaging: comparison of out-of-phase gradient-echo and fat-saturated fast spin-echo techniques—initial experience. *Radiology* 237(2):507–511. <https://doi.org/10.1148/radiol.2372040539>
 20. Cassidy FH, Yokoo T, Aganovic L, Hanna RF, Bydder M, Middleton MS, Hamilton G, Chavez AD, Schwimmer JB, Sirlin CB (2009) Fatty liver disease: MR imaging techniques for the detection and quantification of liver steatosis. *Radiographics* 29(1):231–260. <https://doi.org/10.1148/rg.291075123>
 21. Ma X, Holalkere NS, Kambadakone RA, Mino-Kenudson M, Hahn PF, Sahani DV (2009) Imaging-based quantification of hepatic fat: methods and clinical applications. *Radiographics* 29(5):1253–1277. <https://doi.org/10.1148/rg.295085186>
 22. Longo R, Pollesello P, Ricci C, Masutti F, Kvam BJ, Bercich L, Crocè LS, Grigolato P, Paoletti S, de Bernard B (1995) Proton MR spectroscopy in quantitative in vivo determination of fat content in human liver steatosis. *J Magn Reson Imaging* 5(3):281–285. <https://doi.org/10.1002/jmri.1880050311>
 23. Kleiner DE, Brunt EM, Van Natta M, Behling C, Contos MJ, Cummings OW, Ferrell LD, Liu YC, Torbenson MS, Unalp-Arida A, Yeh M, McCullough AJ, Sanyal AJ, Nonalcoholic Steatohepatitis Clinical Research Network (2005) Design and validation of a histological scoring system for nonalcoholic fatty liver disease. *Hepatology* (Baltimore, MD) 41(6):1313–1321. <https://doi.org/10.1002/hep.20701>
 24. Bedossa P, Poitou C, Veyrie N, Bouillot JL, Basdevant A, Paradis V, Tordjman J, Clement K (2012) Histopathological algorithm and scoring system for evaluation of liver lesions in morbidly obese patients. *Hepatology* (Baltimore, MD) 56(5):1751–1759. <https://doi.org/10.1002/hep.25889>
 25. Mihm S, Fayyazi A, Hartmann H, Ramadori G (1997) Analysis of histopathological manifestations of chronic hepatitis C virus infection with respect to virus genotype. *Hepatology* (Baltimore, MD) 25(3):735–739. <https://doi.org/10.1002/hep.510250340>
 26. Tsochatzis E, Papatheodoridis GV, Manesis EK, Chrysanthos N, Kafiri G, Petraki K, Hadziyannis E, Pandelidaki H, Zafropoulou R, Savvas S, Koskinas J, Archimandritis AJ (2007) Hepatic steatosis in genotype 4 chronic hepatitis C is mainly because of metabolic factors. *Am J Gastroenterol* 102(3):634–641. <https://doi.org/10.1111/j.1572-0241.2006.01025.x>
 27. Rastogi R, Gupta S, Garg B, Vohra S, Wadhawan M, Rastogi H (2016) Comparative accuracy of CT, dual-echo MRI and MR spectroscopy for preoperative liver fat quantification in living related liver donors. *Indian J Radiol Imaging* 26(1):5–14. <https://doi.org/10.4103/0971-3026.178281>
 28. Orlicchio A, Bolacchi F, Cadioli M, Bergamini A, Cozzolino V, Angelico M, Simonetti G (2008) Evaluation of the severity of chronic hepatitis C with 3-T1H-MR spectroscopy. *AJR Am J Roentgenol* 190(5):1331–1339. <https://doi.org/10.2214/AJR.07.2262>
 29. van Werven JR, Marsman HA, Nederveen AJ, Smits NJ, ten Kate FJ, van Gulik TM, Stoker J (2010) Assessment of hepatic steatosis in patients undergoing liver resection: comparison of US, CT, T1-weighted dual-echo MR imaging, and point-resolved 1H MR spectroscopy. *Radiology* 256(1):159–168. <https://doi.org/10.1148/radiol.10091790>
 30. Idilman IS, Keskin O, Celik A, Savas B, Elhan AH, Idilman R, Karcaaltincaba M (2016) A comparison of liver fat content as determined by magnetic resonance imaging-proton density fat fraction and MRS versus liver histology in non-alcoholic fatty liver disease. *Acta Radiol* (Stockholm, Sweden: 1987) 57(3):271–278. <https://doi.org/10.1177/0284185115580488>
 31. Nouredin M, Lam J, Peterson MR, Middleton M, Hamilton G, Le TA, Bettencourt R, Changchien C, Brenner DA, Sirlin C, Loomba R (2013) Utility of magnetic resonance imaging versus histology for quantifying changes in liver fat in nonalcoholic fatty liver disease trials. *Hepatology* (Baltimore, MD) 58(6):1930–1940. <https://doi.org/10.1002/hep.26455>
 32. El-Badry AM, Breitenstein S, Jochum W, Washington K, Paradis V, Rubbia-Brandt L, Puhan MA, Slinkamenac K, Graf R, Clavien PA (2009) Assessment of hepatic steatosis by expert pathologists: the end of a gold standard. *Ann Surg* 250(5):691–697. <https://doi.org/10.1097/SLA.0b013e3181bcd6dd>
 33. Traussnigg S, Kienbacher C, Gajdošik M, Valkovič L, Halilbasic E, Stift J, Rechling C, Hofer H, Steindl-Munda P, Ferenci P, Wrba F, Trattng S, Krššák M, Trauner M (2017) Ultra-high-field magnetic resonance spectroscopy in non-alcoholic fatty liver disease: Novel mechanistic and diagnostic insights of energy metabolism in non-alcoholic steatohepatitis and advanced fibrosis. *Liver Int* 37(10):1544–1553. <https://doi.org/10.1111/liv.13451>
 34. Chalasan N, Wilson L, Kleiner DE, Cummings OW, Brunt EM, Unalp A, NASH Clinical Research Network (2008) Relationship of steatosis grade and zonal location to histological features of steatohepatitis in adult patients with non-alcoholic fatty liver disease. *J Hepatol* 48(5):829–834. <https://doi.org/10.1016/j.jhep.2008.01.016>
 35. Sheikh MY, Choi J, Qadri I, Friedman JE, Sanyal AJ (2008) Hepatitis C virus infection: molecular pathways to metabolic syndrome. *Hepatology* (Baltimore, MD) 47(6):2127–2133. <https://doi.org/10.1002/hep.22269>
 36. Patton HM, Patel K, Behling C, Bylund D, Blatt LM, Vallée M, Heaton S, Conrad A, Pockros PJ, McHutchison JG (2004) The impact of steatosis on disease progression and early and sustained treatment response in chronic hepatitis C patients. *J Hepatol* 40(3):484–490. <https://doi.org/10.1016/j.jhep.2003.11.004>
 37. Neuschwander-Tetri BA, Caldwell SH (2003) Nonalcoholic steatohepatitis: summary of an AASLD Single Topic Conference. *Hepatology* (Baltimore, MD) 37(5):1202–1219. <https://doi.org/10.1053/jhep.2003.50193>
 38. Talaat A, Fatin A, Elsayy A (2012) Hepatic steatosis in HCV infection genotype 4 in Egypt. *Egypt Liver J* 2(1):16–21. <https://doi.org/10.1097/01.ELX.0000403334.90863.91>
 39. Fishbein MH, Gardner KG, Potter CJ, Schmalbrock P, Smith MA (1997) Introduction of fast MR imaging in the assessment of hepatic steatosis. *Magn Reson Imaging* 15(3):287–293. [https://doi.org/10.1016/s0730-725x\(96\)00224-x](https://doi.org/10.1016/s0730-725x(96)00224-x)
 40. Wyatt J, Baker H, Prasad P, Gong YY, Millson C (2004) Steatosis and fibrosis in patients with chronic hepatitis C. *J Clin Pathol* 57(4):402–406. <https://doi.org/10.1136/jcp.2003.009357>

41. Leandro G, Mangia A, Hui J, Fabris P, Rubbia-Brandt L, Colloredo G, Adinolfi LE, Asselah T, Jonsson JR, Smedile A, Terrault N, Paziienza V, Giordani MT, Giostra E, Sonzogni A, Ruggiero G, Marcellin P, Powell EE, George J, Negro F, HCV Meta-Analysis (on) Individual Patients' Data Study Group (2006) Relationship between steatosis, inflammation, and fibrosis in chronic hepatitis C: a meta-analysis of individual patient data. *Gastroenterology* 130(6):1636–1642. <https://doi.org/10.1053/j.gastro.2006.03.014>
42. Anderson N, Borlak J (2008) Molecular mechanisms and therapeutic targets in steatosis and steatohepatitis. *Pharmacol Rev* 60(3):311–357. <https://doi.org/10.1124/pr.108.00001>
43. Modaresi Esfeh J, Ansari-Gilani K (2016) Steatosis and hepatitis C. *Gastroenterol Rep* 4(1):24–29. <https://doi.org/10.1093/gastro/gov040>
44. Cho SG, Kim MY, Kim HJ, Kim YS, Choi W, Shin SH, Hong KC, Kim YB, Lee JH, Suh CH (2001) Chronic hepatitis: in vivo proton MR spectroscopic evaluation of the liver and correlation with histopathologic findings. *Radiology* 221(3):740–746. <https://doi.org/10.1148/radiol.2213010106>

Publisher's Note

Springer Nature remains neutral with regard to jurisdictional claims in published maps and institutional affiliations.

Submit your manuscript to a SpringerOpen[®] journal and benefit from:

- ▶ Convenient online submission
- ▶ Rigorous peer review
- ▶ Open access: articles freely available online
- ▶ High visibility within the field
- ▶ Retaining the copyright to your article

Submit your next manuscript at ▶ [springeropen.com](https://www.springeropen.com)
